Effect of shear on morphology, viability and metabolic activity of succinic acid producing *Actinobacillus succinogenes* biofilms.

Sekgetho Charles Mokwatlo[a], Hendrik Gideon Brink[a], Willie Nicol[a]

Department of Chemical Engineering, University of Pretoria, Lynnwood

Road, Hatfield, 0002, Pretoria, South Africa

Postal address: Department of Chemical Engineering, University of Pretoria, Private Bag X20, Hatfield, 0028, South Africa

E-mail addresses:

Mr. S.C. Mokwatlo: u11119072@tuks.co.za

Dr H.G. Brink: deon.brink@up.ac.za

Prof. W. Nicol: willie.nicol@up.ac.za : corresponding author

Abstract

Two custom designed bioreactors were used to evaluate the effect of shear on biofilms of a succinic acid producer, *Actinobacillus succinogenes*. The first bioreactor allowed for in-situ removal of small biofilm samples used for microscopic imaging. The second bioreactor allowed for complete removal of all biofilm and was used to analyse biofilm composition and productivity. The smooth, low porosity biofilms obtained under high shear conditions had an average cell viability of 79% compared to 57% at the lowest shear used. The maximum cell-based succinic acid productivity for high shear biofilm was 2.4 g g^{-1}DCW h^{-1} compared to the 0.8 g g^{-1}DCW h^{-1} of the low shear biofilm. Furthermore, 3-(4,5-dimethylthiazol-2-yl)-2,5-diphenyl tetrazolium bromide (MTT) assays confirmed higher cell metabolic activities for high shear developed biofilm compared to biofilm developed at low shear conditions. Results clearly indicated that high shear biofilm cultivation has beneficial morphological, viability, and cell-based productivity characteristics.

Keywords: *Actinobacillus succinogenes*; shear; biofilm; productivity; succinic acid

Introduction

Among the US DOE's reported "top value-added chemicals from biomass", succinic acid (SA) is most sought after and well established as a top platform chemical with an estimated market of $132 million in 2018, which is expected grow to $183 million by 2023. Succinic acid finds application in the pharmaceutical industry, in the food industry as pH regulator and flavouring agent, as an ion chelator and surfactant, and mostly as a building block chemical. It is a precursor for a plethora of high value chemicals including 1,4-butanediol, tetrahydrofuran, adipic acid, γ-butyrolactone, and n-methylpyrrolidone. Though conventionally produced via the catalytic hydrogenation of maleic anhydride derived from butane, several companies—BioAmber, Myriant, BASF-Purac and Riverdia—are commercially producing bio-succinic acid via microbial production routes using proprietary microorganisms and pure sugars. This is part of an important drive to transition from a petroleum-based economy to a sustainable biomass-based economy, thereby reducing the impact of the former on the environment.

Various microorganisms have been used for bench-scale fermentation experiments to produce succinic acid. Reported wild type microbes in literature include *Mannheimia succiniciproducens* [1], *Anaerobiospirillum succiniciproducens* [2] *Basfia succiniciproducens* [3], and modified strains of *Escherichia coli* [4]. It is the rumen bacterium *Actinobacillus succinogenes* 130Z however, that is the most apt for industrial bio-succinic acid production, owing mainly to its capacity to produce succinic acid at titres [5–9], productivities, and yields [10–12] well above its competitors. In addition, *A. succinogenes* is reportedly prone to unavoidable formation of biofilms in continuous fermentations [11], which is particularly desirable due to the high cell concentrations attainable in this form. Unlike suspended cells, in biofilms cell aggregates are embedded in a self-produced matrix of gel-like extracellular polymeric substances (EPS). This allows cells to self-adhere to surfaces at high concentrations thereby removing the need to use costly cell retention

strategies for increasing cell concentrations. High cell concentrations are crucial for high volumetric productivities, partly aiding in making bio-succinic production economically feasible. Other beneficial aspects of biofilms are their prolonged stability in long-term processing, and tolerance to toxic substances. Overall, these factors make *A. succinogenes* biofilms a preferable biocatalyst for bulk continuous bio-succinic acid production.

The main challenge with biofilms however is that they have no set properties, their structural and physical characteristics such as density, porosity, thickness, cohesiveness, and cell viability are dictated to a large extent by conditions in which they have been cultivated. Various studies on biofilms have shown that hydrodynamic shear conditions and the specific growth rate of biofilms, among other factors, greatly influence the formation of biofilms, particularly their structure, stability, and the activity of cells embedded in them [13–15]. A previous study, by this research group, investigated the influence of acid accumulation on the development, structure, and viability of *A. succinogenes* biofilms [16]. This study found that high acid conditions (above 10 g L^{-1} SA) impeded biofilm growth and resulted in patchy biofilms with significant cell death, whereas low acid conditions (below 10 g L^{-1} SA) favoured biofilm growth with relatively higher cell viability within biofilms. However, according to literature [13-15], it is expected that hydrodynamic shear conditions (HSC) in bioreactors will also influence the characteristics of biofilms formed by *A. succinogenes*. Most literature report the formation of stronger (dense) and thinner biofilms at high HSC, compared to low HSC where heterogenous, porous, and weaker biofilm structures tend to be formed [17–19]. Moreover, studies in microbial fuel cells have consistently shown that high shear operation resulted in more viable biofilms with increased metabolic activity and high current generation [20]. Therefore, shear variation could potentially impact *A. succinogenes* biofilms in such a way that it improves biofilm viability and ultimately SA productivity. To date no studies have been conducted on the impact of shear variation on the development of *A. succinogenes*

biofilms, particularly looking at the possibility of forming more viable biofilms by varying shear conditions in the fermenter and ultimately increasing total cell-based SA productivity.

The objective of this study was to investigate the role of hydrodynamic shear conditions on the biofilm development of *A. succinogenes* biofilms, specifically assessing the biofilm morphology, cellular viability, and SA cell-based productivity by employing two custom developed bioreactors. The first bioreactor allowed for in-situ removal of small biofilm samples used for microscopic imaging with a confocal scanning laser microscope (CSLM). The second bioreactor allowed for complete removal of all the biofilm and was used to measure biofilm composition and SA cell-based productivity. In this way, the impact of shear was evaluated at a microscopic level in the first bioreactor with respect to the structure and cell activity of biofilms, and at a macroscopic level in the second bioreactor where the SA cell-based productivity of the biofilm and its composition were measured. Succinic acid concentrations were controlled below 10 g L^{-1} in the first bioreactor to favour biofilm growth. Turbine rotational speed was used to vary shear in the first bioreactor (250 & 500 rpm) while the liquid superficial velocity (0.36 & 0.64 m s^{-1}) was used to vary shear in the second bioreactor, both methods have been validated as effective methods to regulate shear rate [18].

2. Materials and Methods

Microorganism and fermentation media

Wild-type *Actinobacillus succinogenes* 130Z (DSM No. 22257; ATCC No. 55618) was acquired from the German Collections of Microorganisms and Cell Cultures (Braunschweig, Germany). Stock cultures (1.5 mL) were stored at −40 °C in 66% v/v glycerol solutions. Inoculum was prepared by transferring a stock culture to 100 mL of sterilised tryptone soy broth at 30 g L^{-1} and incubating at 37 °C and 120 rpm for 16 to 24 h. Prior to inoculation, the inoculum was analysed

for purity by checking for consistent metabolite distribution using High-performance liquid chromatography (HPLC).

The fermentation medium was a replica of the medium developed by Bradfield & Nicol (2014). All chemicals were obtained from Merck KGaA (Darmstadt, Germany) unless otherwise stated. The fermentation medium consisted of three parts: the nutrient and salts solution, a phosphate buffer, and the glucose solution. The nutrient and salt solution was composed of: 10.0 g L^{-1} of clarified corn steep liquor (Sigma-Aldrich, St. Louis, USA), 6.0 g L^{-1} yeast extract, 0.5 g L^{-1} NaCl, 0.2 g L^{-1} $MgCl_2 \cdot 6H_2O$, 0.2 g L^{-1} $CaCl_2 \cdot 2H_2O$, and 10 mL L^{-1} antifoam SE-15 (Sigma-Aldrich, Germany). The phosphate buffer consisted of 3.2 g L^{-1} KH_2PO_4 and 1.6 g L^{-1} K_2HPO_4. The glucose concentration was kept at 60 g L^{-1}. CO_2 (Afrox, South Africa) was fed to the fermenters at 0.1 vvm.

Bioreactors

Two types of bioreactors were used in the study. The first bioreactor (bioreactor A) was custom developed by this research group for the purpose of microscopic visualisation of biofilm development; the details of this reactor was presented in Mokwatlo et al. [16]. The visualisation and analysis of the microscopic biofilm development was facilitated by the extraction of multiple asynchronous sterile samples of biofilm coupons from the bioreactor volume. These coupons could then be studied under a confocal laser scanning microscope (CSLM) to investigate the microscopic architectural differences caused by variation of HSC. HSC were varied by altering the rotating speed (rpm) of the Rushton six blade impeller connected to the overhead stirrer. The maximum speed of the stirrer was 500 rpm. The second bioreactor type (bioreactor B), is a homogenous shear silicone tube bioreactor, presented in the study by Brink & Nicol [12]. Bioreactor B was used for testing the biomass-based succinic acid productivity performance of biofilms developed at varying

HSC as it allowed the complete removal of the developed biofilm for further analysis and quantification. In bioreactor B, HSC conditions were varied by changing the broth superficial velocity within the tube.

In both bioreactors, temperature and pH were controlled at 37.0 ± 0.1 °C and 6.80 ± 0.01 respectively. A Liquiline CM442 (Endress+Hauser, Gerlingen, Germany) coupled to a Ceragel CPS71D glass electrode (Endress+Hauser, Gerlingen, Germany) measured both temperature and pH, and controlled pH by dosing of a 10 M NaOH solution by a peristaltic pump connected to an internal relay. Temperature was controlled by a feedback PID controller, custom developed in Labview. All gas vents and inlets were fitted with 0.2 μm PTFE membrane filters (Midisart 2000, Sartorius, Göttingen, Germany) to ensure sterility.

Biofilm cultivation for visualisation.

Biofilm was cultivated under low acid accumulation conditions (below 10 g L^{-1} SA) in bioreactor A in a similar manner to Mokwatlo et al. [16] except that shear conditions were varied by varying mixing from 250 to 500 rpm. In summary, the bioreactor was initially run in batch mode to facilitate the accumulation of substantial suspended cell biomass (1.86 ± 0.3 g DCW L^{-1}) whilst below 10 g L^{-1} of SA, to avoid cell washout before switching to continuous mode for biofilm cultivation. Subsequently, the biofilm sampling coupons were aseptically inserted into the bioreactor while simultaneously switching to continuous operation mode at a dilution rate of 0.3 h^{-1}. This ensured that the biofilm was cultivated on the coupons (13 mm Thermanox coverslips, Thermo Fisher Scientific, Massachusetts, USA) below the limiting acid concentration from the onset. Acid metabolite concentrations were monitored throughout the biofilm cultivation period to ensure that the low acid conditions were maintained, the concentration profiles are given in (Fig. 1). Mixing was set at 500 rpm (maximum stirrer output) for high shear conditions, this

corresponded to impeller tip velocity of 1.65 m s^{-1} and a local shear velocity of 0.66 m s^{-1} at the biofilm coupon surface considering the results by Madhrani [21] which report that tangential velocities near the wall of stirred tanks were 0.2 to 0.5 of the impeller tip velocity. For low shear conditions, mixing was set at 250 rpm which corresponded to a local shear velocity of 0.33 m s^{-1} at the coupon surface. Biofilm coupons were sampled daily (starting 24 h after insertion of coupon probes) for 3 days and immediately prepared for microscopic viewing. All operational variables were controlled at similar conditions except for shear conditions.

Biofilm image acquisition

The sampled biofilm coupons were stained with Baclight LIVE/DEAD bacterial viability (Thermo Fisher Scientific, USA) stains as described in the study by Mokwatlo et al. [16]. Biofilm images were acquired using a Zeiss LSM 880 laser scanning confocal microscope (Zeiss, Germany). Biofilm samples were observed under a 40× objective lens (Plan-Neofluar 40×/1.3 Oil DIC). Image z-stacks were acquired by taking a series of horizontal *xy* optical scans from the substratum surface to the top of the biofilm section in set steps of 2 μm. The z-stack scans were acquired at random locations on the biofilm coupons. A minimum of 20 image z-stacks per day of sampling were acquired, ensuring that descriptive quantitative parameters of the biofilm are computed based on a biofilm sample area that is representative of the biofilm, as previously determined by [22]. An excitation wavelength of 488 nm was used, and the emission fluorescence was collected at 635 nm and 500 nm.

Image analysis

ZEN 2.3 Lite Image Processor (Zeiss, Germany) and the ImageJ [23] software were used to post process biofilm images prior to quantitative analysis. Post processing involved determining the surface and top section of the biofilm image stack. A Comstat2 digital image analysis software, a

plugin to ImageJ, was used to generate quantitative data of the acquired image z-stacks [24]. The biomass content of the biofilm (μm^3 biomass voxels per μm^2 surface area), the roughness co-efficient parameter, and the average biofilm thickness were computed for each image stack. The descriptions of how each parameter is computed by the Comstat2 software from the biofilm images is reported in [23]. Additionally, the volume porosity of the biofilm was computed using equation (1), as reported by Paranova et al. [19], where *Biovolume* is the volume occupied by bacteria in a 3D image, *Average Thickness* is the average thickness of the biofilm, and *Area Image* is the area of the scanned region.

$$Volume\ Porosity = \left(1 - \frac{Biovolume}{Average\ Thickness \times Area\ Image}\right) \quad (1)$$

The percentage of "alive" cells was calculated by assuming that the total cells were equal to the sum of green and red pixels and further calculating the percentage of green pixels. This calculation was performed for each cross-sectional image scan of each z-stack acquired on the day of sampling and finally averaged to give the mean percentage viability for the day.

Productivity of biofilms developed at varied shear

Investigation of the mass-based productivity of biofilms developed in different shear conditions was conducted using the homogenous shear silicone tube reactor (bioreactor B). Unlike bioreactor A, bioreactor B allowed for the removal and quantification of the entire developed biofilm, and as such the global mass-based succinic acid productivity could be determined. Two shear velocities of 0.36 m s^{-1} and 0.64 m s^{-1} were used from the onset of fermentation. The superficial velocities were chosen to approximately mirror the estimated bulk velocities at the surface of the coupons in bioreactor A. Fermentations were initiated by running the bioreactor in batch mode for 24 h after inoculation to increase the cell concentration. Succinic acid concentration at this point ranged from

10 - 12 g L^{-1} for all the runs. At this point a sufficiently high suspended cell concentration was obtained (2.2 ± 0.3 g DCW L^{-1}) to avoid cell washout, and the fermenter was switched to continuous operation at a dilution rate of 0.9 h^{-1} and 0.2 h^{-1}, for both shear velocities of 0.36 m s^{-1} and 0.64 m s^{-1}. Concentrations of metabolites were monitored until steady state conditions were reached. Steady state was confirmed by a steady average NaOH dosing rate for a 6 h period.

The entire biofilm developed in the homogenous shear tube reactor (bioreactor B) was sampled once steady state conditions were achieved. Prior to biofilm sampling, all the reactor flow streams were stopped, the liquid volume of the bioreactor was removed and noted, and the biofilm was rinsed twice with a phosphate buffered saline (PBS) solution at pH 7 to remove any trace of the broth. The removed reactor broth was replaced with the same volume of the PBS solution. The attached biofilm was completely removed by mechanical friction of the entire silicon tubing, both through the increase of the liquid superficial velocity and externally applied pressure.

Biofilm composition quantification

EPS was extracted from the sampled biofilm using the cation exchange resin (Dowex® Marathon® C sodium form, Sigma-Aldrich, Germany) method as it is reported to result in minimal cell lysis [25]. For separation, 10 mL of the harvested biofilm was poured in a 50 mL Duran bottle with 10 g of cation exchange resin (CER) and a magnetic stirrer. The mixture was then stirred at 600 rpm for 60 min at 4 °C. After allowing for the decanting of the solid CER, the liquid phase was carefully removed and centrifuged at 20000g for 30 min at a temperature of 4 °C. The cell precipitate was then dried in the oven at 70 °C until a constant measured mass remained. The EPS concentrate was analysed for the protein and polysaccharide content. The carbohydrate concentrations of the EPS were determined with the phenol sulfuric acid method using D-glucose

as a standard [26]. Protein content was determined using a Lowry assay method using bovine serum albumin as a standard [27].

MTT analysis

Metabolic activity of biofilm cells was quantified using the MTT method described by Wang et al. [29]. Water-insoluble formazan crystals are formed by the reduction of 3-(4,5-dimethylthiazol-2-yl)-2,5-diphenyl tetrazolium bromide (MTT) by the dehydrogenase system of viable cells in the biofilm. The formazan crystals are then dissolved using DMSO (Sigma-Aldrich, USA) and spectrophotometrically quantified at 550 nm to give a measure of metabolic activity. MTT stock solutions of 5 g L^{-1} were prepared using MTT powder (Sigma-Aldrich, St. Louis, MO) and ultra-purified water, filtered with sterile filters into 2 mL cryogenic vials, and placed in a dark container at −40 ℃ until use.

MTT assays were prepared in triplicates, 20 μL of the MTT stock solution was pipetted into a cuvette, sealed and incubated in the dark at 37 ℃ for 30 min. A 0.2 mL solution of homogenised biofilm sample was added to the cuvettes and further incubated for 60 min at 37 ℃ for the reaction, also in the dark. Consequently, 2 mL of DMSO solution was added to the cuvette solution to dissolve formazan crystals formed, and the dissolution was left for 30 min. Absorbance measurements were then taken at 550 nm to quantify the metabolic activity (T60 UV/VIS Spectrophotometer, PG Instruments, Leicestershire, UK).

Metabolite analysis

Concentrations of glucose and organic acids—succinic acid (SA), acetic acid (AA) and formic acid (FA)— in the fermenter broth were determined by the HPLC [10]. An Agilent 1260 Infinity HPLC (Agilent Technologies, USA), equipped with an RI detector and a 300 mm × 7.8 mm Aminex

HPX-87H ion exchange column (Bio-Rad Laboratories, USA) was used. Two mobile phases were used for two methods of analysis. The first method consisted of a 5 mM H_2SO_4 mobile phase solution fed at a flowrate of 0.6 mL min^{-1} and the second method used a 20 mM H_2SO_4 mobile phase at the same flowrate. The second method improved the accuracy of the glucose reading by separating the phosphate, glucose and pyruvic acid peaks.

3. Results and discussion

Impact of shear on biofilm morphology

Fig. 2 shows top views of the biofilm developed in high shear conditions (Fig. 2 a-c) and low shear conditions (Fig. 2 d-f) from day 1 to day 3 of biofilm cultivation. Biofilm development was expectedly rapid as both low shear and high shear developed biofilms achieved complete surface coverage by the first day of growth (Fig. 2 a&d). However, after a day of cultivation, a marked difference could already be observed in the surface roughness of the developed biofilms. High shear developed biofilms appeared to have a smooth and nearly flat biofilm surface compared to low shear developed biofilms which were rougher with many protuberances of small cell microcolony structures (Fig. 2 a&d). The observations were further confirmed by the quantitative biofilm data; the computed average roughness co-efficient decreased from 0.61 on the first day to as low as 0.03 by day 3 for high shear conditions (Fig. 3a) whereas for low shear biofilms, roughness varied from 0.84 on the first day to 0.52 on day 3 (Fig. 3a). Biofilms cultivated in low shear conditions were initially thicker in comparison to those cultivated in high shear conditions (Fig. 3c). This observation agreed with literature because high shear conditions are often reported to result in thinner biofilms [17-19, 29, 30]. In this way, structurally speaking, high shear conditions physically impacted *Actinobacillus succinogenes* biofilms by constantly eroding biofilm surface thus resulting in thinner and smoother biofilms compared to low shear conditions.

However, by the third day of cultivation the average thickness of low shear biofilms declined to values markedly lower than high shear biofilms (22.9 μm vs 15.3 μm). This was caused by biofilm shedding for low shear conditions as slightly increased biomass in the bioreactor effluent was observed.

Low shear biofilms appeared more porous (Fig. 2 e&f) compared to high shear developed biofilms (Fig. 2 b&c). It was further observed that for high shear biofilms, voids in the biofilms were continually reduced during cultivation so that by day 3 almost no voids could be observed in the structure of the biofilm (Fig 2c). Quantitative data showed that average volume porosity varied from 0.21 to 0.00 and 0.35 to 0.22 for high shear and low shear biofilms respectively (Fig 3b). This suggested that the high shear biofilms were becoming denser (more compact) in comparison to low shear biofilms. Biofilms of *A. succinogenes* thus structurally responded to high shear conditions in a manner that agrees well with other works [18,29,31,32] by forming smooth, less porous biofilms that are more compact and denser compared to those developed at low shear conditions. Compact biofilms are desirable considering the stability of the biocatalyst for extended continuous processing as they are less prone to events of biofilm shedding. This is likely the reason why biofilm shedding was observed in the low shear run but not in the high shear run. However, long operation periods beyond 3 days must be performed to substantiate this observation. In contrast, high biofilm densities can be disadvantageous in that they are widely reported to decrease mass transport of nutrients within the biofilm [18], thus may cause regions of biofilm inactivity due to substrate unavailability in the deeper regions of the biofilm.

Impact of shear on biofilm viability

The biofilm was stained with SYTO9 and propidium iodide of the Baclight Bacterial Viability Kit, this allowed the distinction of “dead” and “alive” cells within the biofilm. Dead cells emitted red

fluorescence whereas living cells emitted green fluorescence. By counting the green and red pixels on each *xy* plane image of a z-stack, it was possible to compute the percentage of "alive cells". The calculation was performed for all the z-stacks collected on a sampling day and averaged to give the mean percentage of "alive" cells in the biofilm for the day. Figure 4 shows the viability results.

High shear conditions resulted in biofilms with a high percentage of "alive" cells throughout the cultivation period, Fig 4a. The average fraction of active cells (over 3 days) for high shear conditions was 79% compared to 57% for low shear cultivated biofilm, though both experienced a decrease in cell viability as the cultivation period progressed. High shear conditions thus improved viable cell content in the biofilm and helped in maintaining a healthy biofilm. It is likely that increased biofilm viability in high shear conditions is a result of shear constantly eroding dead or inactive cellular material. A profile of viable cell fraction across the biofilm depth for 3 randomly selected biofilm z-stacks on day 2 of growth is given in Fig 4b for both low and high shear biofilms. Though high shear biofilms have a markedly higher viability across the biofilm depth compared to low shear biofilms, cell viability decreases slightly (± 10%) towards the deeper layers of the biofilm for both conditions. The slight decrease of cell viability towards the deeper layers of the biofilms may indicate that there were minimal mass transfer effects across the biofilm, even though high developed biofilms were denser.

In Fig. 5 the average viability of biofilms over 3 days are compared for 3 shear conditions (250, 300 & 500 rpm), this includes data from a 300 rpm run reported by Mokwatlo et al. [16]. Results clearly depict that increasing shear conditions in the fermenter leads to the formation of biofilm composed of a high content of viable cells. Average viable cell content increases from 57% to 65%, when mixing intensity is increased from 250 to 300 rpm, and a further increase by 14% in viable cell content when mixing is increased from 300 to 500 rpm. In this way, this study

demonstrates that in addition to shaping the biofilm structure, shear may be employed to improve viable cell content of the developed biofilm. However, it should be noted that increasing shear during biofilm cultivation will at a certain point prevent biofilm formation altogether or result in less biomass concentrations, which is undesirable for high SA volumetric productivities which require high cell concentrations. This was observed where the formation of biofilms at high shear conditions were entirely inhibited at high acid titres (unpublished data). As such there exists trade-offs, and these could not be explored in this study due to the mixing limitation of the employed setup at 500 rpm.

Table 1 statistically compares computed biofilm porosity, roughness and cell viabilities for the two shear conditions employed in this study using a student t-test. The 3-day means are shown to be significantly different in all cases. This further consolidates the observations that shear impacted both the structure and viability of biofilms. Overall, from a microscopic structure perspective, high shear was shown to result in smoother, low porosity biofilms—characteristics which are reportedly tied to stable biofilms—with high content of viable cells.

Impact of shear on biofilm concentration and composition

Reactor B, a tubular reactor, was used to evaluate the effect of shear on the cell-based succinic acid productivity of biofilms structures developed at low shear (0.36 m s^{-1}) and high shear (0.64 m s^{-1}) conditions, as described in the methods section. In addition to this however, the role of shear variation on biofilm composition and viability was also evaluated. Table 2 gives a summary of steady state metabolite and biomass concentrations, steady state was confirmed by a steady average NaOH dosing rate for a 6 h period.

Fermentation runs conducted at low shear conditions (0.36 m s^{-1}) consistently achieved marginally higher total biomass concentrations compared to high shear (0.64 m s^{-1}) runs at similar dilution

rates. For low dilutions of 0.2 h^{-1} a low shear run achieved a total biomass of 9.5 g L^{-1} compared to 8.7 g L^{-1} for a high shear run, whereas at 0.9 h^{-1}, biomass concentrations of 15.4 g L^{-1} and 11.7 g L^{-1} were achieved for low shear and high shear conditions, respectively. Since there is a set surface area within the tube reactor, which was covered by biofilm, it follows that high shear biofilm resulted in thinner biofilms due to lower total biomass concentrations. This ties in well with the microscopic visualisation results. Separating the EPS from the total biomass revealed that low shear runs had a higher fraction of dry cell weight (DCW) compared to high shear runs (Fig. 6). The fraction of cells in the total biomass ranged from 0.77 to 0.85 for low shear runs and from 0.46 to 0.75 for high shear runs. As such, biofilms developed at high flow rates (hence high shear) produced more EPS than low shear biofilms, and this was especially evident at a dilution rate of 0.9 h^{-1} wherein 6.31 g L^{-1} EPS was produced at high shears compared to 2.43 g L^{-1} EPS produced at low shears. The observation agrees with the study by Celmer et al. [18], which reported that high shear conditions induced the overproduction of EPS in biofilms. Since high detachment forces are experienced at high shear conditions, it appears that the biofilm reacted by producing more EPS to strengthen biofilm attachment.

The composition of the EPS was further analysed for polysaccharides and protein content. High shear biofilm EPS contained comparatively more protein than low shear developed biofilm EPS (Fig. 6). Several studies report high protein content in biofilms developed at high shear hydrodynamic conditions [17,18]. Celmer et al. [18] found that high density biofilms were associated with biofilms with a high protein content. Proteins are said to strengthen the biofilm by providing more binding sites [18]. Assuming that high protein content would have the same impact in *A. succinogenes* biofilms, it can be concluded that shear resulted in denser biofilms, which ties in well with microscopic observations of high shear conditions resulting in low porosity and flat biofilms. Dense biofilms are desirable in continuous biofilm processes as they would result in process stabilities due to reduced biofilm sloughing/shedding. Fermenter stability was not

evaluated in this study as biofilm was sampled immediately after steady state conditions were reached. However, in the study by Maharaj et al. [11], frequent instabilities were reported due to biofilm shedding events when the *A. succinogenes* biofilm was cultivated at high dilution rates (low acid titres) and moderate shears.

Impact of shear on biofilm metabolic activity and succinic acid productivity

Estimation of biofilm viability from microscopic images was only based on the sampled biofilm coupons and not the entire biofilm in the fermenter. To consolidate the global and local cell viabilities, a 3-(4,5-dimethylthiazol-2-yl)-2,5-diphenyltetrazolium bromide (MTT) assay was used to assess the relative metabolic activity levels of the entire biofilm developed in bioreactor B at low and high shears. The levels of metabolic active cells are estimated on the principle of the extent of the conversion of MTT to formazan by the dehydrogenase system of viable cells with active metabolism. The formazan absorbance units per milligram dry cell biomass was thus used to compare relative biofilm metabolic activity. Figure 7b, shows that high shear developed biofilm achieved high metabolic activity per dry cell weight for both dilution rates investigated as compared to low shear developed biofilms. This consolidated microscopic results which also showed that high shear biofilm was composed of a higher fraction viable cell. Jones and Buie [34] reported increased metabolic activity with increasing shearing in electroactive biofilms of *Geobacter sulfurreducens*, whereas [35, 36] reported that high shear also induced high metabolic activity in non-electroactive biofilms. This study thus also demonstrates the improved metabolic activity of *A. succinogenes* biofilms by increased hydrodynamic shearing conditions in line with the observations by [34,35,36].

In Figure 7a, mass-based succinic acid productivity for both the low and high shear run are reported. The cellular mass in the biofilm was considered when calculating the cell-based SA

productivity. Biofilms developed in high shear conditions achieved a three-fold higher succinic acid cell-based productivity (2.4 g g^{-1}DCW h^{-1}) compared to that cultivated in low shear conditions (0.81 g g^{-1}DCW h^{-1}) but at the same dilution rate of 0.9 h^{-1}. At the lowest dilution both low and high shear biofilms achieved comparable productivities albeit slightly higher for high shear biofilms. The SA volumetric productivity for high shear developed biofilm (13.3 g $L^{-1}h^{-1}$) was also marginally higher than that of the low shear developed biofilms (10.4 g L^{-1} h^{-1}) for 0.9 h^{-1} dilution rate. Even when considering the total biofilm biomass (DCW & EPS), high shear developed biofilm achieved almost two-fold higher mass-based productivity compared to low shear biofilm.

The results indicate that hydrodynamic shear conditions improved the metabolic activity of the biofilm which was evidenced by the three-fold higher cell-based SA productivity of high shear developed biofilms. This result is supported by the microscopic work which showed that biofilms developed in high shear conditions achieved higher cell viabilities (79%, 3-day average) compared to those developed in low shear conditions (57%, 3-day average), and the MTT assay results which revealed high metabolic activity in biofilms developed at high shears. The improved cell-based productivities are therefore a result of increased levels of active cells in the biofilm and increased metabolic activities caused by operation at increased shear conditions. This work demonstrates that shear plays an important role in continuous fermentations of *Actinobacillus succinogenes* biofilms, by impacting biocatalysts both physically and physiologically.

4. Conclusion

Hydrodynamic shear conditions in a fermenter were shown to have significant impact on the morphology, viability and metabolic activity of *A. succinogenes* biofilms. Biofilms developed in high shear environments were flat, smooth, and less porous than those cultivated at low shear

conditions which tended to be rougher and more porous. The biofilm consisted of a high EPS fraction when cultivated in high shear environments with the proteins constituting a high fraction of the EPS. Since dense and strong biofilms are reported to have a high protein content, it therefore followed that high shear developed biofilms were denser and as a result more stable. Most important however, biofilms developed at high shear conditions were more viable throughout the cultivation period. This translated into high shear developed biofilms exhibiting high cell-based SA productivity, three-fold higher compared to low shear developed biofilms.

Acknowledgements

The Laboratory for Microscopy and Microanalysis at the University of Pretoria is acknowledged for their assistance with the microscope equipment. The financial assistance of the Sugar Milling Research Institute via the Step-Bio program is hereby gratefully acknowledged. The financial assistance of the National Research Foundation (NRF) towards this research is hereby acknowledged. Opinions expressed, and conclusions arrived at, are those of the author and are not necessarily to be attributed to the NRF.

References

[1] Lee PC, Lee SY, Hong SH, Chang HN (2002) Isolation and characterization of a new succinic acid-producing bacterium, *Mannheimia succiniciproducens* MBEL55E, from bovine rumen. Appl Microbiol Biotechnol. https://doi.org/10.1007/s00253-002-0935-6.

[2] Samuelov N, Datta R, Jain M, Zeikus J (1999) Whey fermentation by *Anaerobiospirillum succiniciproducens* for production of a succinate-based animal feed additive. Appl Environ Microbiol 65:2260–2263.

[3] Scholten E, Renz T, Thomas J (2009) Continuous cultivation approach for fermentative succinic acid production from crude glycerol by *Basfia succiniciproducens* DD1. Biotechnol Lett. https://doi.org/10.1007/s10529-009-0104-4.

[4] Beauprez JJ, De Mey M, Soetaert WK (2010) Microbial succinic acid production: Natural versus metabolic engineered producers. Process Biochem. https://doi.org/10.1016/j.procbio.2010.03.035.

[5] Shen N, Zhang H, Qin Y, Wang Q, Zhu J, Li Y, Jiang MG, Huang R (2018) Efficient production of succinic acid from duckweed *(Landoltia punctata*) hydrolysate by *Actinobacillus succinogenes* GXAS137. Bioresour Technol. https://doi.org/10.1016/j.biortech.2017.09.208.

[6] Ferone M, Raganati F, Ercole A, Olivieri G, Salatino P, Marzocchella A (2018) Continuous succinic acid fermentation by *Actinobacillus succinogenes* in a packed-bed biofilm reactor. Biotechnol Biofuels. https://doi.org/10.1186/s13068-018-1143-7.

[7] Ki S, Lin C, Du C, Koutinas A, Wang R, Webb C (2008) Substrate and product inhibition kinetics in succinic acid production by *Actinobacillus succinogenes*. Biochem Eng J. https://doi.org/10.1016/j.bej.2008.03.013.

[8] González-García S, Argiz L, Míguez P, Gullón B (2018) Exploring the production of bio-succinic acid from apple pomace using an environmental approach. Chem Eng J. https://doi.org/10.1016/j.cej.2018.06.052.

[9] Ferone M, Raganati F, Olivieri G, Salatino P, Marzocchella A (2018) Continuous Succinic Acid Fermentation by *Actinobacillus Succinogenes:* Assessment of Growth and Succinic Acid Production Kinetics. Appl Biochem Biotechnol. https://doi.org/10.1007/s12010-018-2846-8.

[10] Bradfield MFA, Nicol W (2014) Continuous succinic acid production by *Actinobacillus succinogenes* in a biofilm reactor: Steady-state metabolic flux variation. Biochem Eng J. https://doi.org/10.1016/j.bej.2014.01.009.

[11] Maharaj K, Bradfield MFA, Nicol W (2014) Succinic acid-producing biofilms of *Actinobacillus succinogenes*: Reproducibility, stability and productivity. Appl. Microbiol. Biotechnol. https://doi.org/10.1007/s00253-014-5779-3.

[12] Brink HG, Nicol W (2014) Succinic acid production with Actinobacillus succinogenes : rate and yield analysis of chemostat and biofilm cultures. https://doi.org/10.1186/s12934-014-0111-6.

[13] van Loosdrecht MCM, Picioreanu C, Heijnen JJ (2006) A more unifying hypothesis for biofilm structures. FEMS Microbiol Ecol. https://doi.org/10.1111/j.1574-

6941.1997.tb00434.x.

[14] Picioreanu C, van Loosdrecht MCM, Heijnen JJ (2000) Two-Dimensional Model of Biofilm Detachment Caused by Internal Stress from Liquid Flow. Biotechnol Bioeng. https://doi.org/10.1002/1097-0290(20000120)72:2<205::AID-BIT9>3.0.CO;2-L

[15] Stoodley P, Yang S, Lappin-Scott H, Lewandowski Z (1997) Relationship between mass transfer coefficient and liquid flow velocity in heterogenous biofilms using microelectrodes and confocal microscopy. Biotechnol Bioeng. https://doi.org/10.1002/(SICI)1097-0290(19971220)56:6<681::AID-BIT11>3.0.CO;2-B.

[16] Mokwatlo SC, Nchabeleng ME, Brink HG, Nicol W (2019) Impact of metabolite accumulation on the structure, viability and development of succinic acid–producing biofilms of *Actinobacillus succinogenes*. Appl Microbiol Biotechnol. https://doi.org/10.1007/s00253-019-09888-8.

[17] Pellicer-Nàcher C, Smets BF (2014) Structure, composition, and strength of nitrifying membrane-aerated biofilms. Water Res. https://doi.org/10.1016/j.watres.2014.03.026.

[18] Celmer D, Oleszkiewicz JA, Cicek N (2008) Impact of shear force on the biofilm structure and performance of a membrane biofilm reactor for tertiary hydrogen-driven denitrification of municipal wastewater. Water Res. https://doi.org/10.1016/j.watres.2008.02.031.

[19] Paramonova E, Kalmykowa OJ, Van Der Mei HC, Busscher HJ, Sharma PK (2009) Impact of hydrodynamics on oral biofilm strength. J Dent Res. https://doi.org/10.1177/0022034509344569.

[20] Shen Y, Wang M, Chang IS, Ng HW (2013) Effect of shear rate on the response of microbial fuel cell toxicity sensor to Cu(II). Bioresour Technol. https://doi.org/10.1016/j.biortech.2013.02.069.

[21] Madhrani DR (2008) Experimental investigation of the fluid velocity distribution in stirred tank reactors equipped with retreat blade impellers using laser doppler velocimetry. New Jersey Institute of technology. https://digitalcommons.njit.edu/cgi/viewcontent.cgi?article=1355&context=theses. Accessed 20 January 2020.

[22] Mokwatlo SC, Nicol W (2017) Structure and cell viability analysis of *Actinobacillus succinogenes* biofilms as biocatalysts for succinic acid production. Biochem Eng J. https://doi.org/10.1016/j.bej.2017.09.013.

[23] Schneider CA, Rasband WS, Eliceiri KW (2012) NIH Image to ImageJ: 25 years of Image Analysis HHS Public Access. Nat Methods. https://doi.org/10.1038/nmeth.2089.

[24] Heydorn A, Nielsen AT, Hentzer M, Givskov M, Ersbøll BK, Molin S (2000) Quantification of biofilm structures by the novel computer program COMSTAT. Microbiology. https://doi.org/10.1099/00221287-146-10-2395.

[25] Jachlewski S, Jachlewski WD, Linne U, Bräsen C, Wingender J, Siebers B (2015) Isolation of Extracellular Polymeric Substances from Biofilms of the Thermoacidophilic Archaeon *Sulfolobus acidocaldarius*. Front Bioeng Biotechnol. https://doi.org/10.3389/fbioe.2015.00123.

[26] Dubois M, Gilles KA, Hamilton JK, Rebers PA, Smith F (1956) Colorimetric Method for

Determination of Sugars and Related Substances. Anal Chem. https://doi.org/10.1021/ac60111a017.

[27] Walker JM, Waterborg JH, Matthews HR (2003) The Lowry Method for Protein Quantitation. Basic Protein Pept Protoc. https://doi.org/10.1385/0-89603-268-x:1.

[28] Wang H, Cheng H, Wang F, Wei D, Wang X (2010) An improved 3-(4,5-dimethylthiazol-2-yl)-2,5-diphenyl tetrazolium bromide (MTT) reduction assay for evaluating the viability of *Escherichia coli* cells. J Microbiol Methods. https://doi.org/10.1016/j.mimet .2010.06.014

[29] Liu Y, Tay JH (2002) The essential role of hydrodynamic shear force in the formation of biofilm and granular sludge. Water Res. 36:1653–65.

[30] Choi YC, Morgenroth E (2003) Monitoring biofilm detachment under dynamic changes in shear stress using laser-based particle size analysis and mass fractionation. Water Sci Technol. 47: 69–76.

[31] Molobela IP, Ilunga FM (2012) Impact of bacterial biofilms: The importance of quantitative biofilm studies. Ann Microbiol. https://doi.org/10.1007/s13213-011-0344-0.

[32] Qi PS, Bin Wang W, Qi Z (2008) Effect of shear stress on biofilm morphological characteristics and the secretion of extracellular polymeric substances. 2nd Int Conf Bioinforma Biomed Eng. https://doi.org/10.1109/ICBBE.2008.363.

[33] Yang J, Cheng S, Li C, Sun Y, Huang H (2019) Shear stress affects biofilm structure and consequently current generation of bioanode in microbial electrochemical systems (MESS).

Front Microbiol. https://doi.org/10.3389/fmicb.2019.00398.

[34] Jones AD, Buie CR (2019) Continuous shear stress alters metabolism, mass transport, and growth in electroactive biofilms independent of surface substrate transport. Sci Rep. https://doi.org/10.1038/s41598-019-39267-2.

[35] Trulear M, Characklis WG (1982) Dynamics of Biofilm Processes. J Water Pollut Control Fed. https://doi.org/10.2307/25041684.

[36] Liu Y, Taylor JH (2001) Metabolic response of biofilm to shear stress in fixed film culture. J Appl Microbiol. https://doi.org/10.1046/j.1365-2672.2001.01244.x.

Figure Captions

Fig. 1: Succinic acid concentration profiles in the fermenter during biofilm cultivation for low and high hydrodynamic shear conditions.

Fig. 2: Biofilm morphology comparison for cultivation at high (500 rpm) shear (a, b and c) and low (250 rpm) shear (d, e and f). The green colour denotes "living or active" cells whereas the red colour denotes "dead" cells in the biofilm. Images are 3D views of the biofilm from the top. White arrows indicate void arears in the biofilm. Scale bar indicates 20 μm.

Fig. 3: Quantitative characterisation of biofilms cultivated for low & high shears. In (**A**) surface roughness co-efficient of biofilms is compared for 3 days of cultivation. The porosity of biofilms is compared in (**B**) and biofilm thickness is compared in (**C**).

Fig. 4: Comparison of biofilm viability for high and low shear biofilms for 3 days of cultivation (A). Percentage viability was computed by counting green (living cells) and red (dead cells) pixels for all images sampled on a particular day of biofilm cultivation. In (**B**), viability variation across biofilm depth is shown for day 2 biofilms for low and high shear conditions.

Fig. 5: 3 day-average biofilm viability comparison for three shear conditions. The 300 rpm shear cultivation data was reported in the study by Mokwatlo et al. [16].

Fig. 6: Biofilm composition characterisation at different shears and dilution rate. The biofilm was partitioned into carbohydrates, proteins and cells, together this gave the total dry biofilm biomass concentration.

Fig. 7: Cell-based succinic acid productivity is compared for biofilm cultivated at low and high shear conditions (A) for 0.2 h^{-1} and 0.9 h^{-1} dilution rates. MTT assays (B) were also compared to indicate differences in metabolic activities of biofilms cultivated at low and high shear condition.

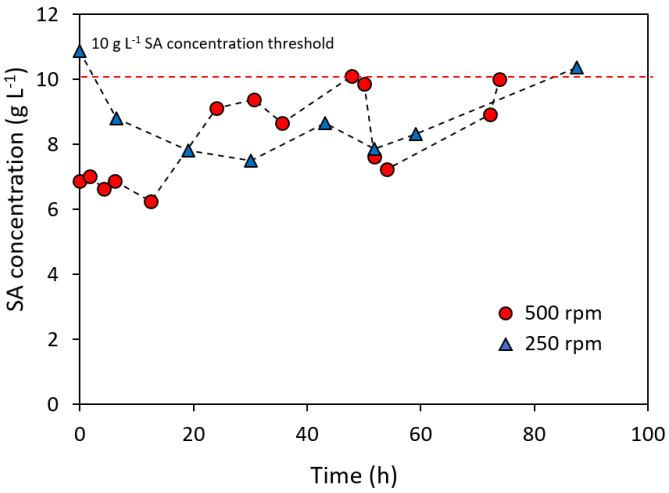

Fig. 1: Succinic acid concentration profiles in the fermenter during biofilm cultivation for low and high hydrodynamic shear conditions.

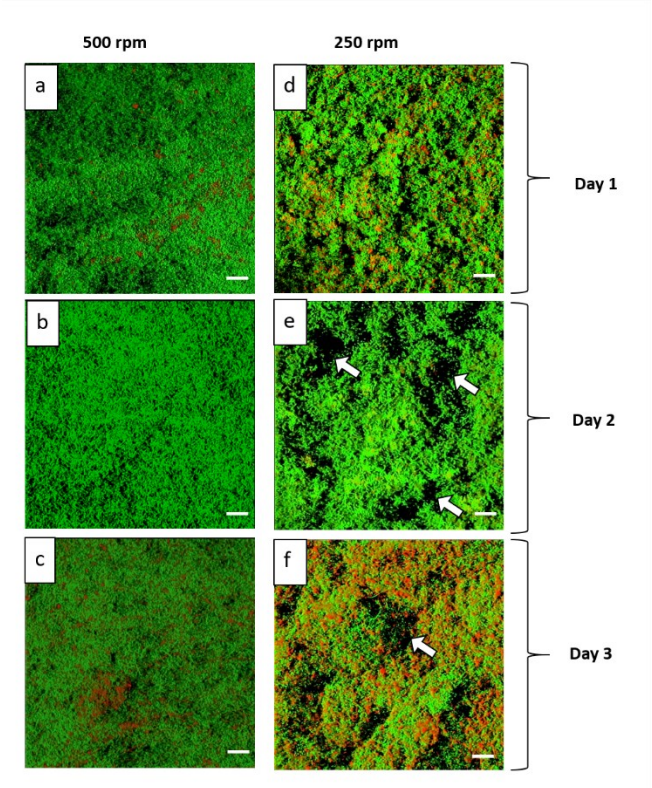

Fig. 2: Biofilm morphology comparison for cultivation at high (500 rpm) shear (a, b and c) and low (250 rpm) shear (d, e and f). The green colour denotes "living or active" cells whereas the red colour denotes "dead" cells in the biofilm. Images are 3D views of the biofilm from the top. White arrows indicate void arears in the biofilm. Scale bar indicates 20 µm.

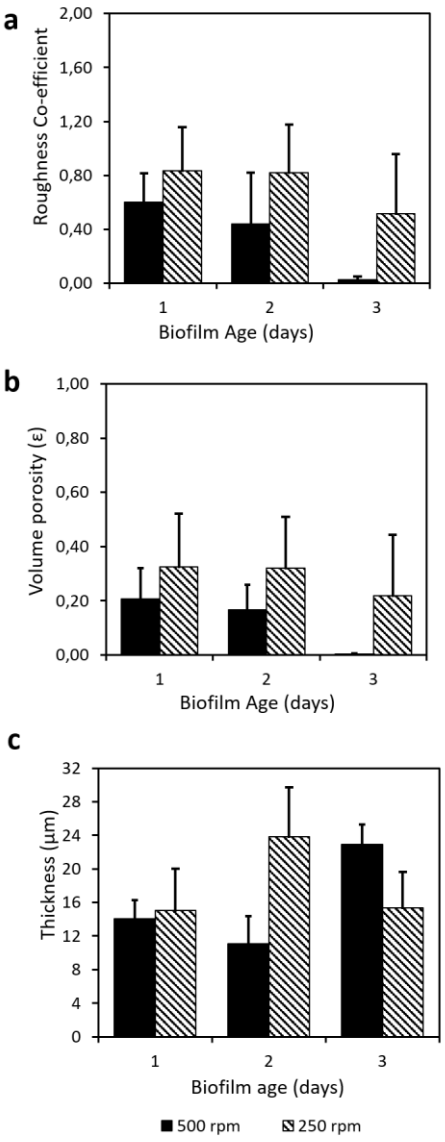

Fig. 3: Quantitative characterisation of biofilms cultivated for low & high shears. In (**A**) surface roughness co-efficient of biofilms is compared for 3 days of cultivation. The porosity of biofilms is compared in (**B**) and biofilm thickness is compared in (**C**).

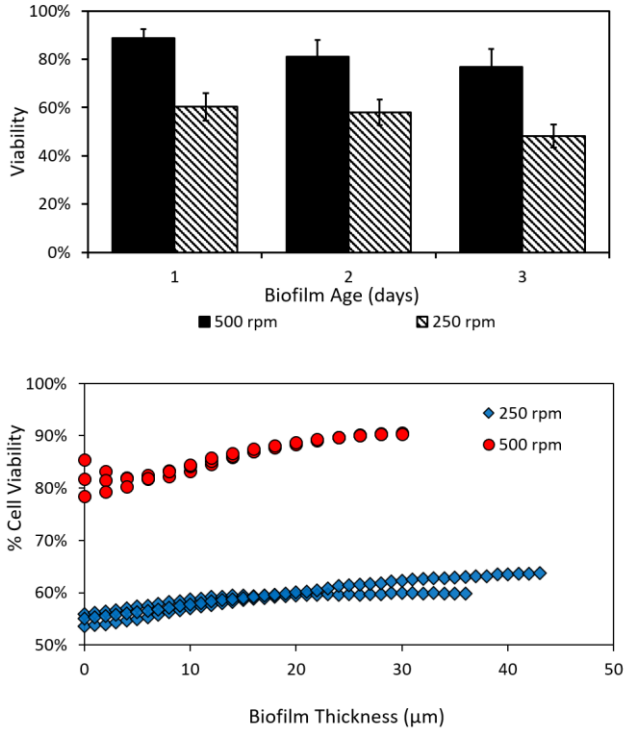

Fig. 4: Comparison of biofilm viability for high and low shear biofilms for 3 days of cultivation (A). Percentage viability was computed by counting green (living cells) and red (dead cells) pixels for all images sampled on a particular day of biofilm cultivation. In (**B**), viability variation across biofilm depth is shown for day 2 biofilms for low and high shear conditions.

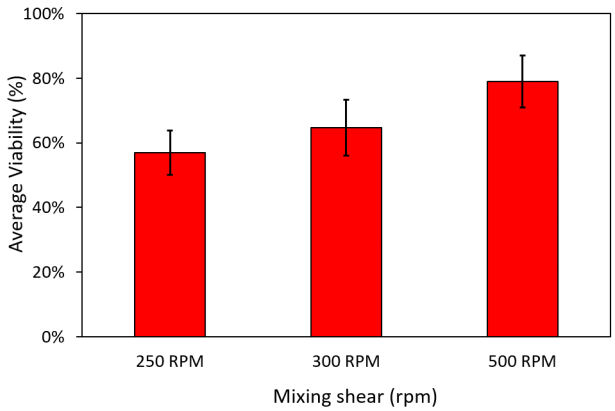

Fig. 5: 3 day-average biofilm viability comparison for three shear conditions. The 300 rpm shear cultivation data was reported in the study by Mokwatlo et al. [16].

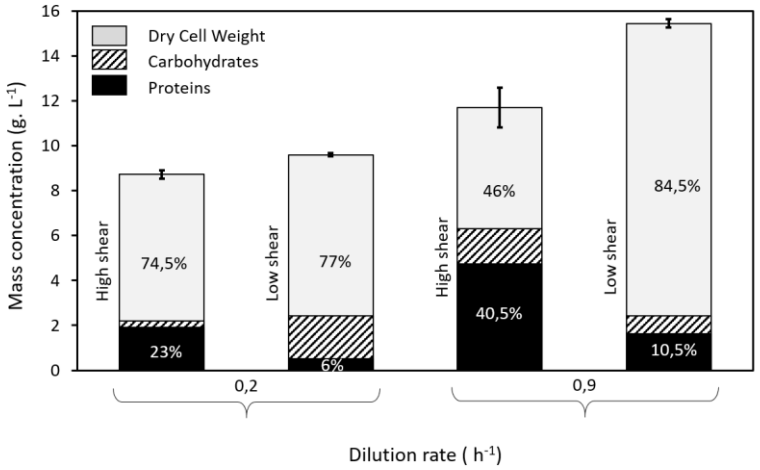

Fig. 6: Biofilm composition characterisation at different shears and dilution rate. The biofilm was partitioned into carbohydrates, proteins and cells, together this gave the total dry biofilm biomass concentration.

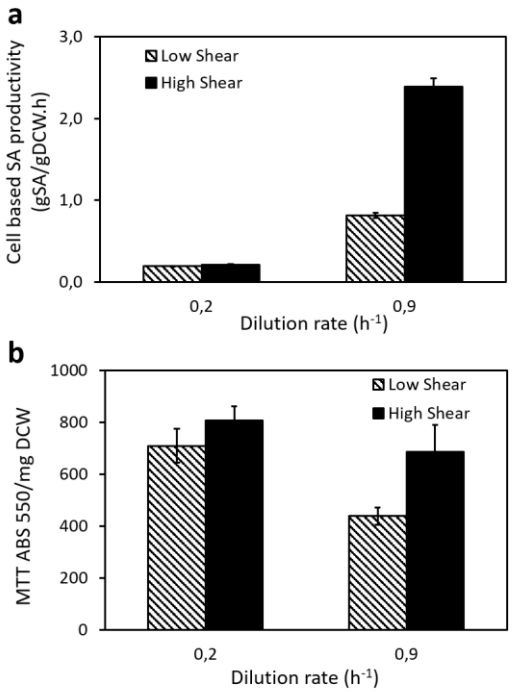

Fig. 7: Cell-based succinic acid productivity is compared for biofilm cultivated at low and high shear conditions (A) for 0.2 h^{-1} and 0.9 h^{-1} dilution rates. MTT assays (B) were also compared to indicate differences in metabolic activities of biofilms cultivated at low and high shear condition.

Table 1: A statistical comparison of biofilm descriptive quantitative parameters.

Parameter	Biofilm Cultivation Conditions		Statistical Comparison		
	500 RPM	250 RPM			
	Mean[1]	Mean	P value	Difference between means	Comment
Roughness Factor	0.314 ± 0.05	0.755 ± 0.051	2.14×10^{-8}	0.440 ± 0.073	Means are significantly different (P< 0.05)
Porosity	0.110 ± 0.022	0.310 ± 0.027	2.26×10^{-8}	0.200 ± 0.036	Means are significantly different (P< 0.05)
Viability	78.98% ± 0.28%	57.00% ± 0.16%	0	21.98% ± 0.3%	Means are significantly different (P< 0.05)

[1] Mean calculated for samples collected over 3 days

Table 2: Steady state fermentation results for biofilm fermentation at varied shear velocities.

Shear velocity ($m\ s^{-1}$)	Run No.	D (h^{-1})	SA ($g\ L^{-1}$)	AA ($g\ L^{-1}$)	FA ($g\ L^{-1}$)	SA/AA	Total Biomass ($g\ L^{-1}$)	Calculated biofilm thickness[1] (μm)
0.36	1	0.9	11.57 ± 0.35[2]	4.77 ± 0.06	2.4 ± 0.08	2.43	15.44 ± 0.04	258
	2	0.2	6.84 ± 0.10	4.19 ± 0.01	1.86 ± 0.01	1.63	9.54 ± 0.06	152
0.64	1	0.9	14.85 ± 0.6	5.6 ± 0.4	2.2 ± 0.2	2.65	11.69 ± 0.54	196
	2	0.2	6.75 ± 0.21	3.86 ± 0.02	2.16 ± 0.01	1.75	8.72 ± 0.4	120

[1] Thickness calculated assuming that dry biomass constitutes 10% of biofilm and uniform biofilm coverage of tubular bioreactor.

[2] Standard deviation calculated for samples taken in triplicates